HHS Public Access

Author manuscript

Sci Signal. Author manuscript; available in PMC 2020 June 01.

Published in final edited form as:

Sci Signal. ; 12(609): . doi:10.1126/scisignal.aaw4956.

Thiol-based direct threat sensing by the stress-activated protein kinase Hog1

Angel Guerra-Moreno[1], **Miguel A. Prado**[2,#], **Jessie Ang**[1,#], **Helena M. Schnell**[1], **Yagmur Micoogullari**[1], **Joao A. Paulo**[2], **Daniel Finley**[2], **Steven P. Gygi**[2], **John Hanna**[1,*]

[1]Department of Pathology, Brigham and Women's Hospital and Harvard Medical School, Boston, Massachusetts, United States of America

[2]Department of Cell Biology, Harvard Medical School, Boston, Massachusetts, United States of America

Abstract

The yeast stress-activated protein kinase Hog1 is best known for its role in mediating the response to osmotic stress, but it is also activated by various mechanistically distinct environmental stressors, including heat shock, endoplasmic reticulum stress, and arsenic. In the osmotic stress response, the signal is sensed upstream and relayed to Hog1 through a kinase cascade. Here, we identified a mode of Hog1 function whereby Hog1 senses arsenic though a direct physical interaction that requires three conserved cysteine residues located adjacent to the catalytic loop. These residues were essential for Hog1-mediated protection against arsenic, dispensable for the response to osmotic stress, and promoted the nuclear localization of Hog1 upon exposure of cells to arsenic. Hog1 promoted arsenic detoxification by stimulating phosphorylation of the transcription factor Yap8, promoting Yap8 nuclear localization, and stimulating the transcription of the only known Yap8 targets, *ARR2* and *ARR3*, both of which encode proteins that promote arsenic efflux. The related human kinases ERK1 and ERK2 also bound to arsenic in vitro, suggesting that this may be a conserved feature of some members of the mitogen-activated protein kinase (MAPK) family. These data provide a mechanistic basis for understanding how stress-activated kinases can sense distinct threats and perform highly specific adaptive responses.

Introduction

All cells utilize stress responses to identify and mitigate toxic threats. Hog1 is an evolutionarily conserved stress-activated protein kinase in *Saccharomyes cerevisiae* and is best known for its role in the osmotic stress response, wherein it orchestrates a complex

*Corresponding Author : jwhanna@bwh.harvard.edu.

#These authors contributed equally.

Author Contributions: J.H. and A.G.M. conceived of the project. A.G.M, J.A., J.H., H.S., and Y.M. carried out the experiments. M.A.P. performed the proteomic aspects of the work, with assistance and supervision from J.A.P., D.F., and S.G. J.H. and A.G.M. wrote the manuscript with input from all the authors.

Competing Interests: The authors declare that they have no competing interests.

Data and Materials Availability: The proteomics data have been deposited to the ProteomeXchange Consortium via the PRIDE partner repository (data set identifier PXD015325) and are also available upon request. All other data needed to evaluate the conclusions in the paper are present in the paper or the Supplementary Materials.

program of cellular remodeling (1). Hog1 controls the transcription of ~600 genes, and this is achieved in large part through Hog1-dependent phosphorylation of transcription factors. Hog1 also has important non-transcriptional functions, including regulation of key membrane proteins (2). Hog1 is related to a family of mammalian mitogen-activated protein kinases (MAPKs) and is generally considered to be the yeast ortholog of the p38 family of MAPKs, which function in a wide variety of cellular processes.

In addition to osmotic stress, Hog1 is also activated by various mechanistically distinct environmental stressors including heat shock, hypoxia, tunicamycin, and arsenic, suggesting a broad role for Hog1 in cellular stress responses (3).The mechanistic basis for Hog1 activation by such diverse stressors remains poorly understood. Similarly, it is unclear whether Hog1 can generate distinct cellular responses for each of these stressors. Arsenic, particularly in its trivalent form (arsenite), is a ubiquitous environmental toxin with broad public health relevance. Exposure is associated with multiple types of cancer as well as an increased risk of diabetes (4–6), and arsenic currently ranks first on the U.S. Superfund Substance Priority List (7). An important aspect of arsenic toxicity relates to its ability to covalently interact with free thiol groups in amino acid side chains (8–10), and this protein-modifying capacity may underlie its ability to induce proteotoxic stress (11–13). The ubiquitous nature of arsenic toxicity is underscored by the observation that cells from bacteria to humans have developed mechanisms to deal with arsenic toxicity (4). Remarkably, trivalent arsenic is also a highly effective FDA-approved therapy for acute promyelocytic leukemia; in combination with a second drug (all-*trans* retinoic acid), it has helped transform this cancer from one that was typically fatal to one in which cure rates now exceed 90% (14). This cancer is driven by a cytogenetic translocation–derived fusion protein, PML-RARα. Arsenic covalently binds to free thiol groups in this fusion protein, triggering destruction of the protein by the ubiquitin-proteasome system (15).

Previous work suggests that the function of Hog1 in the arsenic stress response is likely to be quite different from that in the context of osmotic stress. Hog1 is typically phosphorylated in response to stress (16). However, arsenic induces only modest phosphorylation of Hog1 compared to osmotic stress (17). Moreover, the broad transcriptional changes seen after osmotic stress are not seen after arsenic treatment, suggesting either a more limited transcriptional response or perhaps even no transcriptional response (18).

Given arsenic’s capacity to covalently modify cysteine residues, we sought to test the hypothesis that thiol-based regulation by arsenic might contribute to Hog1 function in response to this stress. We identified three evolutionarily conserved cysteine residues that were required for Hog1’s role in protecting cells from arsenic but completely dispensable for the osmotic stress response. The mechanistic basis for this cysteine-based regulation appeared to be direct binding of arsenic to Hog1. We used quantitative proteomics approaches to understand the outcome of this thiol-based regulation. Our data suggest that Hog1 promoted arsenic detoxification through Yap8, which is itself an arsenic-binding protein and an exquisitely specific transcription factor that has only two known targets. These two target genes are transcribed from a single bidirectional promoter, and the proteins they encode, Arr2 and Arr3, mediate arsenic efflux.

This work provides insight into a fundamental aspect of cellular signaling – how cells can sense individual threats and carry out highly specific adaptive responses. The capacity of Hog1 to bind arsenic appears to be evolutionarily conserved: it was also observed with the human MAPKs ERK1 and ERK2, both of which show absolute conservation of these cysteine residues. Given that many stressors are capable of altering thiol chemistry, thiol-based regulation may represent an important new direction in the study of Hog1 and its mammalian orthologs.

Results

Three cysteine residues in Hog1 specifically protect against arsenic toxicity

Hog1 contains six cysteine residues (Fig. 1A). Four of these residues (Cys^{38}, Cys^{156}, Cys^{161}, Cys^{205}) show a high degree of evolutionary conservation from yeast to humans. We introduced single Cys-to-Ser mutations at each of the four sites and expressed these Hog1 substitution mutants from the endogenous *HOG1* promoter in a low-copy centromeric vector in the *hog1Δ* background. The plasmid encoding wild-*type HOG1* fully complemented the null mutant's sensitivity to arsenic (Fig. 1B). Three of the mutants (C156S, C161S, and C205S) showed some sensitivity to arsenic (Fig. 1B), whereas the C38S mutant did not. We expressed a C156/205S double mutant and a C156/161/205S triple mutant (hereafter referred to as the "3C mutant"). Both showed strong sensitivity to arsenic, comparable to the null mutant (Fig. 1B). To determine whether this was a specific effect, we assayed the canonical and best-established function of Hog1: protection against osmotic stress. The *hog1Δ* mutant showed sensitivity to osmotic stress, as expected (Fig. 1B). Remarkably, however, none of the cysteine point mutants showed any growth defect, suggesting a specific role for these cysteine residues in the arsenic stress response (Fig. 1B; fig. S1). This effect could not be attributed to a difference in protein abundance, because the wild-type and Hog1–3C proteins showed no difference in abundance by immunoblot (Fig. 1C).

Key cysteine residues in Hog1 mediate direct binding to arsenic

The kinase activity of Hog1 and of its related kinases in higher organisms is mediated by a central catalytic loop and an adjacent activation segment (Fig. 2A). The three cysteine residues we identified as important for the response to arsenic (Cys^{156}, Cys^{161}, and Cys^{205}) are well-positioned to potentially regulate Hog1 function, being located just adjacent to the catalytic loop and the activation segment (Fig. 2A). A key feature of arsenic toxicity relates to its ability to covalently interact with free thiol groups in amino acid side chains. Trivalent arsenic, in particular, may be coordinated by three cysteine residues (19). Therefore, we sought to determine whether Hog1 might be regulated by direct arsenic binding to these residues.

To measure arsenic binding, we used a biotinylated form of trivalent arsenic (hereafter As-Bio) which can be purified by affinity chromatography. We prepared clarified cell extracts, treated them with As-Bio, and purified material bound to As-Bio. As an internal positive control, we assayed Yap8, which is the best characterized arsenic-binding protein in yeast (Fig. 2B) (19). We readily detected wild-type Hog1 in the eluates; by contrast, binding of Hog1–3C was attenuated (Fig. 2B). The strength and specificity of the Hog1-arsenic

interaction are indicated in two ways. First, the resins were washed in buffer containing 4M urea, which would be expected to eliminate weak or non-specific interactions. Second, the As-Bio probe has a molecular weight of 427 daltons, and we were able to detect a corresponding shift in the eluted Hog1 protein relative to the input material (Fig. 2B). These findings strongly suggest covalent binding of arsenic to Hog1. Next, we pre-treated lysates with unlabeled arsenic and repeated the binding assay. Binding of Hog1 to the As-Bio probe was attenuated in the pre-treated sample (Fig. 2C). Finally, we pre-treated cells with unlabeled arsenic and repeated the binding assay. Again, binding of Hog1 to the As-Bio probe was strongly attenuated in the pre-treated sample (Fig. 2D). Because the unlabeled arsenic had only been present in vivo (the cells were extensively washed prior to lysis), this provides strong evidence that Hog1 bound to arsenic in vivo.

Thiol-based regulation of Hog1 promotes arsenic detoxification by the transcription factor Yap8

To gain insight into the function of these critical cysteine residues in Hog1, we carried out a quantitative proteomic analysis of *hog1Δ* cells expressing the wild-type or Hog1–3C mutant before and after arsenite treatment using tandem mass tag–based (TMT) mass spectrometry. This method's increased capacity for multiplexing allowed us to perform this analysis with biologic duplicates (no treatment) or triplicates (arsenite treatment). We quantified 4,574 proteins (of ~6000 in yeast), indicating a comprehensive analysis. Unexpectedly, the differences between the two strains were relatively limited (Fig. 3A; fig. S2, A and B; Table S3). Only 110 proteins showed a difference in arsenic-dependent induction using $p<0.01$ as a threshold for statistical significance. Very few of these proteins showed large-magnitude differences.

Among proteins that were not properly induced in the *hog1–3C* mutant, the top hit was Arr2 (Fig. 3A-B). In yeast, arsenic export is mediated by a three-gene regulon (*ARR1, ARR2,* and *ARR3*; ref. (20). Arr2 functions as an arsenate reductase, reducing pentavalent arsenate to trivalent arsenite. Trivalent arsenite can then be exported by the plasma membrane protein Arr3. There is little or no production of Arr2 and Arr3 under normal conditions. Arsenic exposure strongly stimulates transcription of the genes and is mediated by the AP1-like transcription factor Yap8 (also called Arr1), which recognizes a bidirectional promoter located between *ARR2* and *ARR3* (figs. S3 and S4, A and B; refs. 21-22). This pathway of arsenic detoxification is exquisitely specific: Yap8 has no other known transcriptional targets, and the only other potential transport substrate of Arr3 besides arsenite is the closely related metalloid antimony (22–23). Furthermore, direct binding of arsenic to Yap8 is required for its transcriptional stimulatory function, providing a molecular explanation for its ability to sense arsenic (Fig. 2B; ref. 19). Arr3 was also one of the top hits in the proteomic analysis and showed reduced arsenite-dependent induction in the *hog1–3C* mutant, similar to Arr2 (Fig. 3A-B). No peptides from Yap8 were detected in the proteomic analysis.

To confirm these results for Arr2 and Arr3, we inserted sequences encoding a 3xHA tag at the 3'-end of each gene. These proteins were thus expressed from their endogenous genomic loci and without alteration of their upstream promoter elements. We cultured cells and prepared whole cell extracts before and after arsenite treatment. We analyzed the extracts by

SDS-PAGE followed by immunoblotting with antibodies specific for HA. Both Arr2 and Arr3 were strongly induced in the wild-type strain after arsenic treatment (Fig. 3, C and D; fig. S5, A and B). By contrast, the *hog1–3C* mutant showed a significant defect in inducing both Arr2 and Arr3. The fact that both proteins were affected in the *hog1–3C* mutant suggested that a defect in Yap8-dependent transcription might be the cause. To test this model, we performed RT-PCR. Similar to the immunoblotting data, both *ARR2* and *ARR3* were induced by arsenic in the wild-type strain, but this transcriptional induction was strongly abrogated in the *hog1–3C* mutant (Fig. 3E fig. S5C).

The preceding data suggest an exceptionally specific arsenic sensor and effector function for Hog1. Using three conserved cysteine residues, Hog1 directly bound arsenic and in turn stimulated perhaps the most specific aspect of the cellular response to arsenic, which is the program of arsenic detoxification mediated by Yap8. Cysteine oxidation, for example by sulfenylation or disulfide bond formation, is known to regulate the function of some proteins in response to oxidative stress (24–26), and arsenic itself is known to be a potent oxidizing agent (9). However, a key feature of Yap8 is its exquisite specificity: it is activated by arsenic but not by other oxidizing agents (Fig. 3F). Thus, generic oxidation of Hog1 cysteine residues would likely not provide the specificity required for Hog1's ability to stimulate Yap8 activity, and highlights the utility of direct arsenic binding to Hog1 (Fig. 2).

Hog1 promotes nuclear localization of Yap8

The transcriptional function of Yap8 requires nuclear localization, which has been previously observed upon arsenic treatment of cells (21–22). However, there have been conflicting results with regard to Yap8 localization in the absence of arsenic. One group has reported that it is predominantly cytoplasmic (21), whereas another has reported it to be constitutively nuclear (22). We used fluorescence microscopy to determine the localization of green fluorescent protein–tagged endogenous Yap8 (GFP-Yap8). In the absence of arsenic stress, the Yap8 signal was weak, consistent with its known arsenic-dependent accumulation (27). In *hog1Δ* cells expressing wild-type Hog1, we observed strong nuclear localization after arsenic treatment (Fig. 4A), consistent with the prior reports, and this was confirmed by co-localization with mCherry-tagged histone H2B. This co-localization was markedly attenuated in *hog1Δ* cells expressing the Hog1–3C mutant (Fig. 4A-B), wherein Yap8 accumulated in a punctate location that was adjacent to but not co-localized with histone H2B (Fig. 4A). This most likely represents a perinuclear or cytoplasmic structure adjacent to the nucleus. Thus, Hog1 exerted its stimulatory effect on Yap8 function at least in part through promoting or maintaining nuclear Yap8 localization in the presence of arsenic.

Yap8 undergoes Hog1-dependent phosphorylation

Hog1 is known to directly phosphorylate many of its targets, including several transcription factors (3). Thus, Hog1-dependent phosphorylation of Yap8—either direct or indirect—could represent a straightforward model for regulation. Yap8 has not previously been reported to be phosphorylated. To detect potential phosphorylation of Yap8, we used Phos-tag, a manganese-based reagent that binds phospho-groups, resulting in a mobility shift that can be detected by standard SDS-PAGE and immunoblotting (28–29). After treatment of cells with arsenic, we observed a robust mobility shift of the Yap8 protein, consistent with

phosphorylation (Fig. 4C). This mobility shift was strongly attenuated in the *hog1–3C* mutant (Fig. 4C; fig. S6). The small amount of residual Yap8 phosphorylation in the *hog1–3C* mutant could reflect either residual activity in this mutant or partial redundancy with another kinase. To determine whether the defect in Yap8 phosphorylation in the *hog1–3C* mutant was specific, we looked at the phosphorylation of an osmotic stress-induced Hog1 target, the transcription factor Sko1 (30). Sko1 phosphorylation upon high salt stress was retained in the *hog1–3C* mutant (fig. S7), consistent with the lack of phenotypic sensitivity of this mutant to osmotic stress (Fig. 1B; fig. S1).

Yap8 contains 45 serine and threonine residues. Some of these sites are potentially compatible with the Hog1 consensus sequence (S/T-P), but redundancy of Hog1-mediated phosphorylation sites is well documented, making identifying candidate phosphorylation sites a major challenge (30). Through multiple rounds of site-directed mutagenesis, we were able to obtain a Yap8 mutant protein containing 7 serine or threonine–to-alanine substitutions (7-Ser/Thr) that, when expressed in the *yap8*Δ mutant, showed comparable abundance to the wild-type protein in the absence of arsenic, but was largely deficient in arsenic-induced phosphorylation (Fig. 4D). The *yap8*Δ mutant expressing this 7-Ser/Thr mutant protein showed strong sensitivity to arsenic treatment (Fig. 4E), indicating that phosphorylation was critical for Yap8 function. Consistent with this finding, the Yap8 phosphorylation-deficient mutant showed a strong, although not complete, reduction in arsenite-induced expression of *ARR2* and *ARR3* (fig. S8). Finally, the reduced abundance of the arsenite-induced phosphorylated Yap8 species in the 7-Ser/Thr mutant (Fig. 4E), as well as the presence of a small but detectable amount of Phos-tag dependent band shift in non-arsenite-treated samples (Figs. 4C and 5B), make it unlikely that the shifted band reflects an unanticipated effect of arsenic binding.

Cells expressing Hog1–3C show additional evidence of a defect in arsenic detoxification

As noted above (Fig. 3A), of proteins that showed deficient induction by arsenic in the *hog1Δ* cells expressing Hog1–3C, Arr2 was the most severely affected. Conversely, there was a small number of proteins that showed excessive induction in these cells. Among the most affected was Rpn4 (Fig. 3A; fig. S9A), a transcription factor that controls the abundance of proteasomes in response to stress. Under conditions that inhibit or overwhelm proteasome function, Rpn4 accumulates and stimulates new proteasome production (31). Once protein-degrading capacity has been restored, Rpn4 is itself subject to degradation, normalizing the response (13). We examined this normalization of Rpn4 abundance after stress by immunoblotting. In wild-type cells, Rpn4 abundance spiked after arsenic treatment, but returned to near baseline within three hours (fig. S9B). By contrast, normalization of Rpn4 abundance was markedly attenuated in the *yap8Δ* mutant (fig. S9B). Thus, the excessive induction of Rpn4 in cells expressing Hog1–3C (Fig. 3A, fig. S9A) is consistent with a defect in arsenic detoxification by Yap8. Arr2 and Arr3 are also indicators of arsenic toxicity: their amounts should rise in response to increasing intracellular arsenic concentration. In principle, then, the amounts of Rpn4 and Arr2/3 in cells should tend to track in the same direction, and there are probably very few perturbations that would cause them to track in opposite directions, as they do in cells expressing Hog1–3C. A deficiency of Yap8 function is fully consistent with the divergent response of Arr2/3 and Rpn4.

Hog1 phosphorylation and arsenic-binding are jointly required for stimulation of Yap8

All known functions of Hog1 require its phosphorylation at two evolutionarily conserved residues, Thr^{174} and Tyr^{176} (32). These sites are located within the activation segment, which is near the central catalytic loop (Fig. 2A). In response to osmotic stress, a large increase in Hog1 phosphorylation is noted within minutes and is directly mediated by the upstream kinase Pbs2 (16). In response to arsenic, Hog1 is also phosphorylated, but the extent of phosphorylation is much less than that seen in response to osmotic stress (17). Two models could account for this difference. First, phosphorylation is indeed necessary for Hog1 function in response to arsenic, but only a small fraction of the total Hog1 protein is needed for the response. Second, phosphorylation may be largely dispensable for certain Hog1 functions in response to arsenic.

To distinguish between these models, we prepared a phosphorylation-deficient mutant of Hog1 containing two substitutions (T174A/Y176F). As expected, this mutant was completely deficient in osmostress-induced phosphorylation (fig. S10). We found that arsenic-induced accumulation of Arr3 was strongly attenuated in *hog1Δ* cells expressing Hog1-T174A/Y176F, comparable to the defect seen in *hog1Δ* cells expressing Hog1–3C (Fig. 5A; fig S11A). Arsenite-induced phosphorylation of Yap8 was similarly compromised in the cells expressing Hog1-T174A/Y176F (Fig. 5B; fig S11B). Consistent with these results, cells expressing Hog1-T174A/Y176F were sensitive to both osmotic stress and arsenite treatment, whereas cells expressing Hog1–3C were sensitive only to arsenite (Fig. 5C). Thus, both phosphorylation and cysteine-based regulation are required for Hog1 to promote Yap8 function in response to arsenic.

Arsenic promotes the nuclear localization of Hog1

We sought to understand how arsenic binding regulates Hog1 function. We examined the subcellular localization of GFP-tagged Hog1 (32). Upon arsenite treatment, a large fraction of cells showed nuclear accumulation of Hog1, and this effect was strongly abrogated in *hog1Δ* cells expressing Hog1–3C (Fig. 6A-B). By contrast, wild-type Hog1 and the Hog1–3C mutant accumulated equally in the nucleus upon osmotic stress, indicating the specificity of this effect for arsenic toxicity (Fig. 6A-B).

Previous studies have emphasized the lack of nuclear accumulation of Hog1 upon arsenic treatment relative to that occurring upon osmotic stress, although Hog1 was certainly not excluded from the nucleus in those studies (17–18). We also treated cells with arsenic for a longer time period before visualizing Hog1 than in those studies. Thus, we sought to determine whether the observed nuclear accumulation of Hog1 was physiologically relevant. To do this, we employed a version of Hog1 that is tethered to the plasma membrane, Hog1-CCAAX, thus preventing translocation of Hog1 to the nucleus (Fig. 6C; ref. 2). This mutant fully complemented the growth defect of the *hog1Δ* mutant upon osmotic stress, indicating its general functionality (2). In contrast, *hog1Δ* cells expressing membrane-tethered Hog1 showed strong sensitivity to arsenic exposure, indicating that Hog1 performs an essential non-cytoplasmic function in the presence of arsenic (Fig. 6D). In the osmotic stress response, Hog1 nuclear localization is further promoted by interaction with some of its transcription factor targets (3). We sought to determine if this might also be the case for

Hog1 and Yap8. However, nuclear localization of Hog1 after arsenic treatment was unaffected by loss of Yap8 (Fig. 6E).

Arsenite sensitivity of *hog1* mutants persists in an *mtq2*Δ mutant

Recent evidence suggests that methylation of intracellular arsenite contributes to its toxicity, and loss of the major methyltransferase, Mtq2, confers arsenite resistance (33). We therefore sought to determine whether inhibition of arsenite methylation could impact the protective role of Hog1 in responding to arsenite stress. Both *hog1Δ* mutants and *hog1Δ* mutants expressing Hog1–3C retained their strong sensitivity to arsenite in the *mtq2Δ* background (fig. S12), indicating that at least some critical functions of Hog1 are independent of Mtq2-mediated arsenite methylation.

Arsenic binding may be conserved in mammalian MAPKs

Hog1 is related to a family of mammalian MAPKs that includes p38 (α–δ isoforms), JNK1, JNK2, JNK3, ERK1, ERK2, and ERK5. Traditionally, Hog1 has been thought to be most closely related to the p38 family, although it shows considerable sequence homology to all ten of these mammalian kinases (1). We wanted to determine whether arsenic binding might be a conserved aspect of mammalian MAPK function, a possibility that has not been reported, although some of these proteins are known to function in response to arsenite (34). We used the As-Bio probe to purify proteins from two different human cells lines: Ramos (a Burkitt lymphoma–derived cell line) and U937 (a histiocytic lymphoma cell line). Using an antibody that recognizes p38α and p38β, we did not detect any binding of the As-Bio probe to these proteins (Fig. 7A-B). By contrast, an antibody that detects the closely related kinases ERK1 and ERK2, indicated that both proteins in both cell lines bound to arsenic (Fig. 7A-B).

Sequence analysis of these proteins revealed that the three cysteines we identified in Hog1 are fully conserved in ERK1 and ERK2, but not in p38α or p38β, wherein the second of the three cysteines was not conserved (Fig. 7C). Overall, Hog1 shows a slightly higher sequence homology to p38 than to ERK1/2. However, when considering the central core of these proteins (encompassing the ~100 residues that include the catalytic loop, the activation segment, the phosphorylation sites, and the cysteine residues), Hog1 is actually more closely related to ERK1/2 than it is to p38 (Fig. 7C; fig. S13). The full cysteine triad was not present in any of the other six human MAPKs.

Discussion

A newly identified sensor-effector paradigm for Hog1

Hog1 is best known for its role in the osmotic stress response, but it also responds to a variety of other structurally and mechanistically distinct environmental stressors. How a single kinase like Hog1 can respond to such diverse threats is an important unanswered question. A related question is whether Hog1 can orchestrate distinct effector programs for each of these stressors. Using trivalent arsenic, we identified a previously unrecognized mode of Hog1 function whereby Hog1 directly senses this stressor through its interaction with conserved cysteine residues located near the Hog1 catalytic loop and activation

segment. This binding allows Hog1 to control the most specific aspect of the cellular response to arsenic, the detoxification program mediated by Yap8. Hog1 stimulated Yap8 function, increasing the expression of the only two known Yap8 targets, *ARR2* and *ARR3*. Critical aspects of this regulatory control include Hog1's ability to influence the cellular localization and phosphorylation state of Yap8. At present we do not know whether the Hog1-dependent phosphorylation of Yap8 is direct or indirect. Future efforts to reconstitute this process in vitro should answer that question.

Two prior studies found that transcription of *ARR3* was strongly reduced in the *hog1Δ* mutant, supporting the results reported here (17, 33). Prior work also indicates a non-transcriptional role for Hog1 in the arsenic stress response, because Hog1 negatively regulates the function of the plasma membrane glycerol transporter Fps1, which also mediates arsenic import (18). Thus, similar to the situation in osmotic stress, Hog1 appears to perform multiple functions within the arsenic stress response. Arsenite, moreover, may additionally stimulate Hog1 function by inhibiting the phosphatases Ptp2 and Ptp3, both of which negatively regulate Hog1 activity (33).

Regulation of Hog1 activity by arsenic binding

An important question is why arsenic binding to Hog1 is necessary when Yap8 itself binds arsenic (19). The simple answer is that this Hog1-dependent regulation provides for more effective expression of *ARR2* and *ARR3* (Fig. 3C-E), and the resulting enhanced protection against arsenic toxicity would likely have been selected for over time. A key aspect of arsenic-mediated regulation of Hog1 appears to be its ability to promote stress-specific nuclear accumulation of Hog1. How arsenic does this remains an important question for future work. Other pathways of thiol-based regulation are known to control interaction of the nuclear transport machinery with target proteins (26). It is possible that a similar mode of regulation might apply to Hog1.

A second important consideration is the manner and stoichiometry by which arsenic engages Hog1. Whether the critical residues in Hog1 coordinately bind a single arsenic molecule or can each engage separate arsenic molecules remains to be determined. For Yap8, which shows a strikingly similar distribution of its own three key cysteine residues (Cys^{132}, Cys^{137}, and Cys^{274}), the available evidence suggests equimolar binding (19).

Cysteine-based regulation as broad signaling modality

Recent years have witnessed tremendous progress in the identification of cysteine-based posttranslational modifications in diverse proteins. These include multiple oxidation states (such as that induced by sulfenylation), alkylation, nitrosylation, glutathionylation, and others (24–26, 35). Our data show how cysteine modification upon exposure to arsenic can result in a very specific effector response. Other stressors may result in different modifications of these cysteine residues, such as sulfenylation or nitrosylation, that in turn could result in different signaling outputs. In this sense, these cysteine residues could represent a versatile signaling platform for diverse stress conditions. Some evidence already points in this direction. Two papers, one in fission yeast and the other in *Candida albicans,* have shown that two of these three cysteine residues (Cys^{156} and Cys^{161}) are necessary for

the response to nitrosative or oxidative stress, respectively, although the mechanistic details remain poorly understood (36–37). This more expansive model of thiol-based regulation for Hog1 suggests a potential basis for understanding how stress-activated protein kinases can coordinate highly signal-specific responses at both the sensor and effector levels.

Materials and Methods

Yeast strains, human cell lines, and plasmids

Yeast strains and plasmids are listed in tables S1 and S2, respectively. Standard techniques were used for strain construction and plasmid transformation. Cells were cultured at 30°C. YPD medium consisted of 1% yeast extract, 2% Bacto-peptone, and 2% dextrose. YPGal medium contained 2% galactose instead of dextrose. Plasmid selection was by either supplementation of rich media with ClonNAT (100 μg/ml) or omission of uridine from synthetic media, as appropriate. Note that C-terminal 3xHA tagging of Yap8 did not support wild-type arsenic resistance; therefore, an N-terminal tag was used for immunoblot analysis and fluorescence microscopy.

pJH62 is a low-copy centromeric plasmid derived from ycPlac22 (38) in which the *TRP1* marker has been replaced with the NAT-MX6 cassette, allowing for selection by ClonNAT resistance (39). Site-directed mutagenesis was performed using the QuikChange method (Agilent). Mutations were verified by sequencing.

Human cell lines (U937 and Ramos) were cultured in suspension under standard conditions.

Sodium arsenite (Sigma) was used at 1 mM or less, a standard concentration in yeast (17–18, 21, 33). We previously showed that cells retained viability under these conditions for up to (at least) four hours (13). Indeed, within just 1–2 hours after drug wash-out, the cells resumed growth with a normal doubling time, indicating that the cellular responses observed during treatment are likely to be physiologically relevant and specific to arsenic toxicity, rather than reflecting non-specific toxicity in dead or dying cells (13).

Proteomic analysis

Proteomic analysis was performed by the tandem mass tag-based (TMT) mass spectrometry method as previously described (13). Cells were sampled before (biologic duplicates) and after (biologic triplicates) treatment with sodium arsenite (1 mM for 1 h). 4,574 proteins were quantified (table S3). The proteomics data have been deposited to the ProteomeXchange Consortium via the PRIDE partner repository with the data set identifier PXD015325.

Immunoblotting

Whole cell lysates were prepared from logarithmic phase cultures. Cells were normalized by optical density and collected by centrifugation. Pellets were resuspended in lithium acetate (2 M) and incubated on ice for 5 min, followed by treatment with sodium hydroxide (0.4 M) for 5 min on ice. After centrifugation, pellets were resuspended in Laemmli buffer and boiled at 100°C for 5 min. Standard SDS-PAGE and immunoblotting were performed.

The following antibodies were used in this study: anti-HA-peroxidase (Roche; #12013819001), anti-Pgk1 (Novex; #459250), anti-Hog1 (Santa Cruz; #sc-165978), anti-phospho-38 MAPK T180/Y182 (Cell Signaling, #9211S), anti-Rpn4 (40), anti-p38α/β (Santa Cruz; #sc-7972), and anti-Erk1/Erk2 (Millipore #06–182). Phosphorylation was detected using Phos-tag (Wako #300–93523), a manganese-based reagent that complexes with phosphate groups allowing detection of a size shift by immunoblotting (28–29).

RT-PCR

Reverse-transcription PCR was performed as previously described (41). *YAP8* was amplified using the primers 5'-CGGAACATTAGTAAGGCCTG-3' and 5'-CGGAACATTAGTAAGGCCTG-3'; *ARR2* with 5'-CATAACGTCTAGGCAACTCAAG-3' and 5'-GGTTACTCTCTCTACAATGGG-3'; *ARR3* with 5'-GTCCCATTGGTGCTTTACTTC- and 5'-CCCAAATGTTGCAGCTATTGC-3'; and *ACT1* with 5'-CTGGTATGTTCTAGCGCTTG-3' and 5'- GATACCTTGGTGTCTTGGTC-3'.

Phenotypic analysis

Overnight yeast cultures were normalized by optical density and spotted in a three-fold serial dilution series on the indicated plates and cultured at 30°C for the indicated times.

Biotinylated arsenic binding assay

Logarithmically growing cells were resuspended in lysis buffer (100 mM Tris pH 8, 10% glycerol, 5 mM TCEP, phosphatase inhibitors [1 mM sodium fluoride, 0.5 mM sodium pyrophosphate, and 0.5 mM of sodium orthovanadate], and protease inhibitors [Roche]) and lysed by bead beating. Clarified extracts were treated with biotinylated arsenic (20 μM; Toronto Research Chemicals #B394970) or DMSO for 90 min at 4°C. Samples were diluted 10-fold in urea buffer (10 mM Tris pH8, 4 M urea, 100 mM NaCl, 100 mM Na_2HPO_4, 10% glycerol, 0.1% NP-40), mixed with 50 μl of streptavidin-agarose beads (Sigma #S1638), and incubated for 90 min at 4°C. Resins were washed with 100 bed volumes of urea buffer, and eluted by adding 50 μl of 2X Laemmli buffer and boiling for 10 min.

For the *in vitro* arsenic competition assay, pretreatment was with excess unlabeled sodium arsenite (400 μM) for 30 min. For the *in vivo* arsenic competition assay, one culture was pretreated with sodium arsenite (1 mM) for 1 h. Cells were washed twice with 20 ml of sterile water to remove arsenic from the media prior to lysis.

Fluorescence microscopy

Logarithmically growing cells were treated with sodium arsenite (1 mM for the indicated times), harvested, and washed twice in PBS. Confocal microscopy was performed on live cells. mCherry-tagged Htb2 (histone H2B) was used for nuclear localization. Images were acquired at 1000X magnification under oil and processed using NIH ImageJ software.

Statistical analysis

Statistical analysis, where indicated, was by standard deviation or student's T-test. Significance for the proteomic data (Fig. 3A) was set using a relatively stringent cut-off of $p<0.01$.

Supplementary Material

Refer to Web version on PubMed Central for supplementary material.

Acknowledgments

The authors thank Dr. Lucia Suarez-Lopez for helpful advice and comments on the manuscript; Dr. Korneel Grauwet for technical assistance; Drs. David G. Quintana and Jeremy Thorner for strains and helpful advice; Dr. Randy King for comments on the manuscript; and the BRMC Confocal Microscopy Core Facility.

Funding: This work was supported by NIH grants DP5-OD019800 (to J.H.), K01-DK098285 (to J.P.), R01-GM067945 (to S.G.), and R01-GM43601 (to D.F.).

References and Notes

1. De Nadal E, Posas F. Osmostress-induced gene expression--a model to understand how stress-activated protein kinases (SAPKs) regulate transcription. FEBS J. 2015 9;282(17):3275–85. [PubMed: 25996081]
2. Westfall PJ, Patterson JC, Chen RE, Thorner J. Stress resistance and signal fidelity independent of nuclear MAPK function. Proc Natl Acad Sci U S A. 2008 8 26;105(34):12212–7. [PubMed: 18719124]
3. Saito H, Posas F. Response to hyperosmotic stress. Genetics. 2012 10;192(2):289–318. [PubMed: 23028184]
4. Rosen BP, Liu Z. Transport pathways for arsenic and selenium: a minireview. Environ Int. 2009 4;35(3):512–5. [PubMed: 18789529]
5. Maull EA, Ahsan H, Edwards J, Longnecker MP, Navas-Acien A, Pi J, Silbergeld EK, Styblo M, Tseng CH, Thayer KA, Loomis D. Evaluation of the association between arsenic and diabetes: a National Toxicology Program workshop review. Environ Health Perspect. 2012 12;120(12):1658–70. [PubMed: 22889723]
6. Bonini MG, Sargis RM. Environmental Toxicant Exposures and Type 2 Diabetes Mellitus: Two Interrelated Public Health Problems on the Rise. Curr Opin Toxicol. 2018 2;7:52–59. [PubMed: 29392186]
7. Agency for Toxic Substances and Disease Registry, Centers for Disease Control. Substance Priority List, 2017 https://www.atsdr.cdc.gov/spl/
8. Rosen BP, Bhattacharjee H, Shi W. Mechanisms of metalloregulation of an anion-translocating ATPase. J Bioenerg Biomembr. 1995 2;27(1):85–91. [PubMed: 7629056]
9. Hughes MF. Arsenic toxicity and potential mechanisms of action. Toxicol Lett. 2002 7 7;133(1):1–16. [PubMed: 12076506]
10. Shen S, Li XF, Cullen WR, Weinfeld M, Le XC. Arsenic binding to proteins. Chem Rev. 2013 10 9;113(10):7769–92. [PubMed: 23808632]
11. Pan X, Reissman S, Douglas NR, Huang Z, Yuan DS, Wang X, McCaffery JM, Frydman J, Boeke JD. Trivalent arsenic inhibits the functions of chaperonin complex. Genetics. 2010 10;186(2):725–34. [PubMed: 20660648]
12. Jacobson T, Navarrete C, Sharma SK, Sideri TC, Ibstedt S, Priya S, Grant CM, Christen P, Goloubinoff P, Tamás MJ. Arsenite interferes with protein folding and triggers formation of protein aggregates in yeast. J Cell Sci. 2012 11 1;125(Pt 21):5073–83. [PubMed: 22946053]
13. Guerra-Moreno A, Isasa M, Bhanu MK, Waterman DP, Eapen VV, Gygi SP, Hanna J. 2015 Proteomic Analysis Identifies Ribosome Reduction as an Effective Proteotoxic Stress Response. J Biol Chem. 290, 29695–706. [PubMed: 26491016]
14. Rice KL, de Thé H. The acute promyelocytic leukaemia success story: curing leukaemia through targeted therapies. J Intern Med. 2014 7;276(1):61–70. [PubMed: 24635409]
15. Zhang XW, Yan XJ, Zhou ZR, Yang FF, Wu ZY, Sun HB, Liang WX, Song AX, Lallemand-Breitenbach V, Jeanne M, Zhang QY, Yang HY, Huang QH, Zhou GB, Tong JH, Zhang Y, Wu JH,

Hu HY, de Thé H, Chen SJ, Chen Z. Arsenic trioxide controls the fate of the PML-RARalpha oncoprotein by directly binding PML. Science. 2010 4 9;328(5975):240–3. [PubMed: 20378816]

16. Brewster JL, de Valoir T, Dwyer ND, Winter E, Gustin MC. An osmosensing signal transduction pathway in yeast. Science. 1993 3 19;259(5102):1760–3. [PubMed: 7681220]
17. Sotelo J, Rodríguez-Gabriel MA. Mitogen-activated protein kinase Hog1 is essential for the response to arsenite in Saccharomyces cerevisiae. Eukaryot Cell. 2006 10;5(10):1826–30. [PubMed: 16920868]
18. Thorsen M, Di Y, Tängemo C, Morillas M, Ahmadpour D, Van der Does C, Wagner A, Johansson E, Boman J, Posas F, Wysocki R, Tamás MJ. The MAPK Hog1p modulates Fps1p-dependent arsenite uptake and tolerance in yeast. Mol Biol Cell. 2006 10;17(10):4400–10. [PubMed: 16885417]
19. Kumar NV, Yang J, Pillai JK, Rawat S, Solano C, Kumar A, Grøtli M, Stemmler TL, Rosen BP, Tamás MJ. Arsenic Directly Binds to and Activates the Yeast AP-1-Like Transcription Factor Yap8. Mol Cell Biol. 2015 12 28;36(6):913–22. [PubMed: 26711267]
20. Bobrowicz P, Wysocki R, Owsianik G, Goffeau A, Ułaszewski S. Isolation of three contiguous genes, ACR1, ACR2 and ACR3, involved in resistance to arsenic compounds in the yeast Saccharomyces cerevisiae. Yeast. 1997 7;13(9):819–28. [PubMed: 9234670]
21. Menezes RA, Amaral C, Delaunay A, Toledano M, Rodrigues-Pousada C. Yap8p activation in Saccharomyces cerevisiae under arsenic conditions. FEBS Lett. 2004 5 21;566(1–3):141–6. [PubMed: 15147884]
22. Wysocki R, Chéry CC, Wawrzycka D, Van Hulle M, Cornelis R, Thevelein JM, Tamás MJ. The glycerol channel Fps1p mediates the uptake of arsenite and antimonite in Saccharomyces cerevisiae. Mol Microbiol. 2001 6;40(6):1391–401. [PubMed: 11442837]
23. Maciaszczyk-Dziubinska E, Wawrzycka D, Sloma E, Migocka M, Wysocki R. The yeast permease Acr3p is a dual arsenite and antimonite plasma membrane transporter. Biochim Biophys Acta. 2010 11;1798(11):2170–5. [PubMed: 20655873]
24. Hourihan JM, Moronetti Mazzeo LE, Fernández-Cárdenas LP, Blackwell TK. Cysteine Sulfenylation Directs IRE-1 to Activate the SKN-1/Nrf2 Antioxidant Response. Mol Cell. 2016 8 18;63(4):553–566. [PubMed: 27540856]
25. Guerra-Moreno A, Ang J, Welsch H, Jochem M, Hanna J. Regulation of the unfolded protein response in yeast by oxidative stress. FEBS Lett. 2019 4 19 [Epub ahead of print]
26. Wood MJ, Storz G, Tjandra N. Structural basis for redox regulation of Yap1 transcription factor localization. Nature. 2004 8 19;430(7002):917–21. [PubMed: 15318225]
27. Di Y, Tamás MJ. Regulation of the arsenic-responsive transcription factor Yap8p involves the ubiquitin-proteasome pathway. J Cell Sci. 2007 1 15;120(Pt 2):256–64. [PubMed: 17200139]
28. Ishiai M, Kitao H, Smogorzewska A, Tomida J, Kinomura A, Uchida E, Saberi A, Kinoshita E, Kinoshita-Kikuta E, Koike T, Tashiro S, Elledge SJ, Takata M. FANCI phosphorylation functions as a molecular switch to turn on the Fanconi anemia pathway. Nat Struct Mol Biol. 2008 11;15(11):1138–46. [PubMed: 18931676]
29. Kinoshita E, Kinoshita-Kikuta E, Takiyama K, Koike T. Phosphate-binding tag, a new tool to visualize phosphorylated proteins. Mol Cell Proteomics. 2006 4;5(4):749–57. [PubMed: 16340016]
30. Proft M, Pascual-Ahuir A, de Nadal E, Ariño J, Serrano R, Posas F. Regulation of the Sko1 transcriptional repressor by the Hog1 MAP kinase in response to osmotic stress. EMBO J. 2001 3 1;20(5):1123–33. [PubMed: 11230135]
31. Xie Y, Varshavsky A. RPN4 is a ligand, substrate, and transcriptional regulator of the 26S proteasome: a negative feedback circuit. Proc Natl Acad Sci U S A. 2001 3 13;98(6):3056–61. [PubMed: 11248031]
32. Ferrigno P, Posas F, Koepp D, Saito H, Silver PA. Regulated nucleo/cytoplasmic exchange of HOG1 MAPK requires the importin beta homologs NMD5 and XPO1. EMBO J. 1998 10 1;17(19):5606–14. [PubMed: 9755161]
33. Lee J, Levin DE. Intracellular mechanism by which arsenite activates the yeast stress MAPK Hog1. Mol Biol Cell. 2018 8 1;29(15):1904–1915. [PubMed: 29846136]

34. Huang C, Ma WY, Li J, Goranson A, Dong Z. Requirement of Erk, but not JNK, for arsenite-induced cell transformation. J Biol Chem. 1999 5 21;274(21):14595–601. [PubMed: 10329651]

35. Lo Conte M, Carroll KS. The redox biochemistry of protein sulfenylation and sulfinylation. J Biol Chem. 2013 9 13;288(37):26480–8. [PubMed: 23861405]

36. Day AM, Veal EA. Hydrogen peroxide-sensitive cysteines in the Sty1 MAPK regulate the transcriptional response to oxidative stress. J Biol Chem. 2010 3 5;285(10):7505–16. [PubMed: 20061379]

37. Herrero-de-Dios C, Day AM, Tillmann AT, Kastora SL, Stead D, Salgado PS, Quinn J, Brown AJP. Redox Regulation, Rather than Stress-Induced Phosphorylation, of a Hog1 Mitogen-Activated Protein Kinase Modulates Its Nitrosative-Stress-Specific Outputs. MBio. 2018 3 27;9(2). pii: e02229–17.

38. Gietz RD, Sugino A. 1988 New yeast-Escherichia coli shuttle vectors constructed with in vitro mutagenized yeast genes lacking six-base pair restriction sites. Gene. 74, 527–34. [PubMed: 3073106]

39. Jochem M, Ende L, Isasa M, Ang J, Schnell H, Guerra-Moreno A, Micoogullari Y, Bhanu M, Gygi SP, Hanna J. Targeted Degradation of Glucose Transporters Protects against Arsenic Toxicity. Mol Cell Biol. 2019 4 30;39(10). pii: e00559–18.

40. Guerra-Moreno A, Hanna J. Induction of proteotoxic stress by the mycotoxin patulin. Toxicol Lett. 2017 7 5;276:85–91. [PubMed: 28529145]

41. Guerra-Moreno A, Hanna J. 2016 Tmc1 Is a Dynamically Regulated Effector of the Rpn4Proteotoxic Stress Response. J Biol Chem. 291, 14788–95. [PubMed: 27226598]

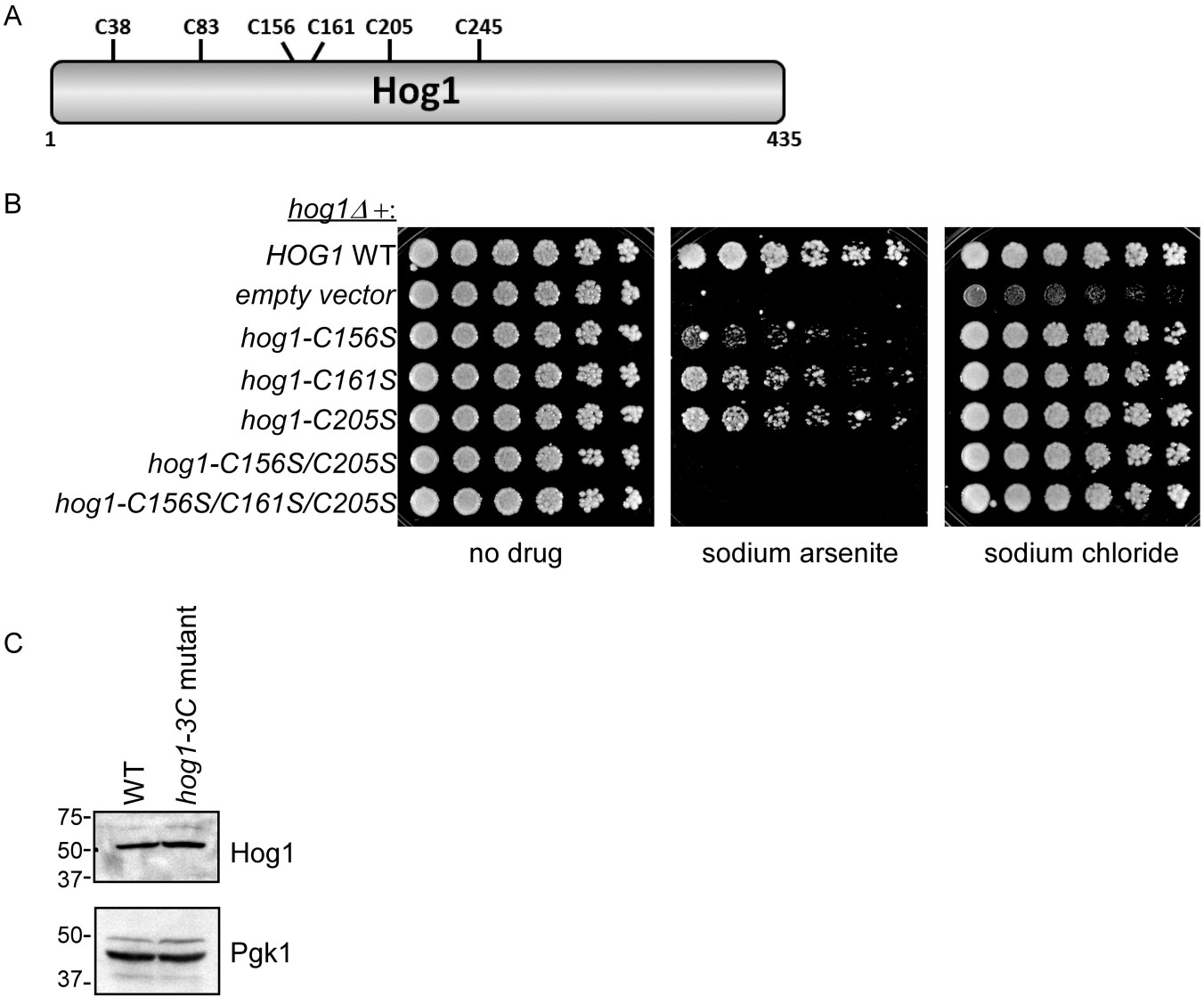

Fig. 1. Key cysteine residues in Hog1 are required for the response to arsenite.

(**A**) Schematic representation of the Hog1 protein with cysteine (C) residues noted. (**B**) Yeast cells lacking Hog1 (*hog1Δ*) and expressing the indicated proteins were spotted in three-fold serial dilutions on media containing no drug, sodium arsenite (1 mM), or sodium chloride (0.4 M) and cultured for 2–3 days. Results are representative of at least three independent experiments. (**C**) Steady-state abundance of WT Hog1 and Hog1–3C in *hog1Δ* cells expressing one or the other protein, as determined by SDS-PAGE and immunoblotting. Pgk1 is a loading control. Similar results were obtained in two independent experiments (see also table S3).

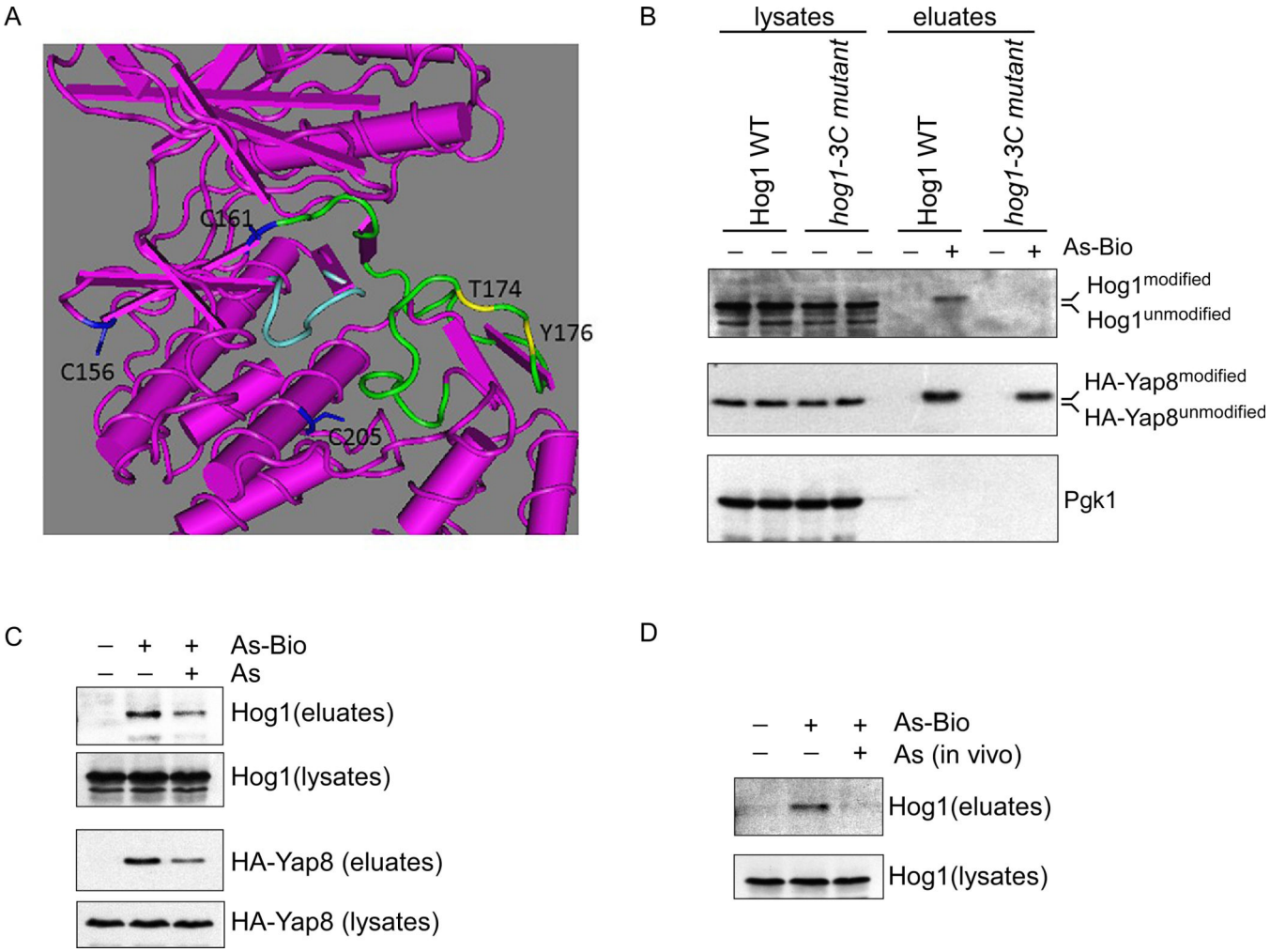

Fig. 2. Arsenic binding to Hog1 requires three key cysteine residues.

(**A**) Structural features of Hog1, as modeled on the conserved MAPK ERK2 (PDB: 5NHV). Cyan, catalytic loop; green, activation segment; yellow, phosphorylation sites; blue, the three cysteine residues identified in this work. Residue numbering is according to yeast Hog1. (**B**) Binding of arsenic to wild-type (WT) Hog1 and the Hog1–3C mutant, as determined by streptavidin affinity purification using a biotinylated arsenic probe (As-Bio; 20 μM) in lysates of *hog1Δ* cells expressing HA-tagged Yap8 and either WT Hog1 or Hog1–3C. Eluates were analyzed by SDS-PAGE and immunoblotting for Hog1 and HA. Note that binding of As-Bio causes a slight increase in the size of the protein which can be seen relative to the untreated lysate proteins. Pgk1 is a loading control for total lysates and a negative control for arsenic binding. Similar results were obtained in more than three independent experiments. (**C**) Binding of As-Bio to WT Hog1 in the presence of excess unlabeled arsenite. The experiment was performed similarly to that in (B), except that unlabeled arsenite (400 μM) was added prior to addition of As-Bio. Proteins were immunoblotted for Hog1 and HA-Yap8. Similar results were obtained in three experiments. (**D**) Binding of biotinylated arsenic to WT Hog1 isolated form cells that had been previously treated with unlabeled arsenite (1 mM for 1 h). Cells were extensively washed prior to lysis,

ensuring that unlabeled arsenic was only present in vivo. Proteins were immunoblotted for Hog1 and HA-Yap8. Similar results were obtained in three experiments.

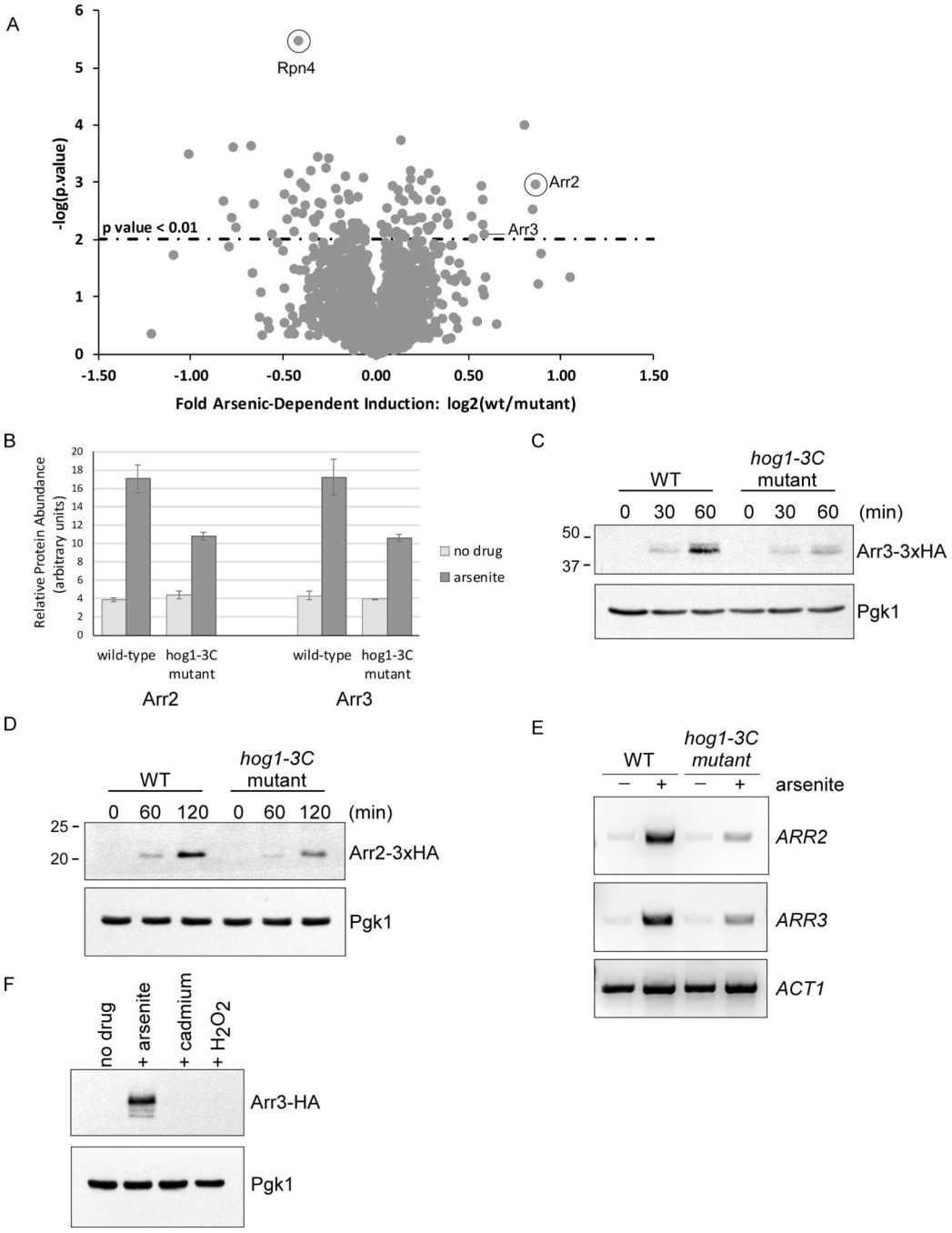

Fig. 3. Hog1 promotes arsenic detoxification by stimulating the activity of the transcription factor Yap8.

(**A**) Proteomic analysis of the arsenite stress response in *hog1Δ* cells expressing WT Hog1 or Hog1–3C, as determined by tandem mass tag-based mass spectrometry. Cells were sampled before and after sodium arsenite treatment (1 mM for 1 hour). The fold arsenic-dependent induction is expressed as the ratio of WT to mutant. Hits with positive value show attenuated induction in the mutant, whereas hits with negative value show enhanced induction in the mutant. The Y-axis represents statistical significance, as determined by two-

tailed student's T test. (**B**) Abundance of Arr2 and Arr3, as determined by the proteomic analysis in panel A. Error bars reflect standard deviations from biologic duplicates (no drug) or triplicates (arsenite treatment). (**C-D**) Induction of Arr2 and Arr3 protein after sodium arsenite treatment (1 mM) in *hog1Δ* cells expressing an HA-tagged form of either Arr2 (C) or Arr3 (D) from the endogenous locus plus either WT Hog1 or Hog1–3C, as determined by SDS-PAGE and immunoblotting for HA. Pgk1 is a loading control. Similar results were obtained in at least three experiments. (**E**) Transcriptional induction of *ARR2* and *ARR3* after sodium arsenite treatment in *hog1Δ* cells expressing WT or Hog1–3C mutant, as determined by RT-PCR. *ACT1* is a control. Similar results were obtained in at least three experiments. (**G**) Immunoblotting for HA in whole-cell lysates from yeast expressing HA-tagged Arr3 from the endogenous locus and treated for 90 min with sodium arsenite (1 mM), cadmium chloride (100 mM), or hydrogen peroxide (6.5 mM). Pgk1 is a loading control. Similar results were obtained in three experiments.

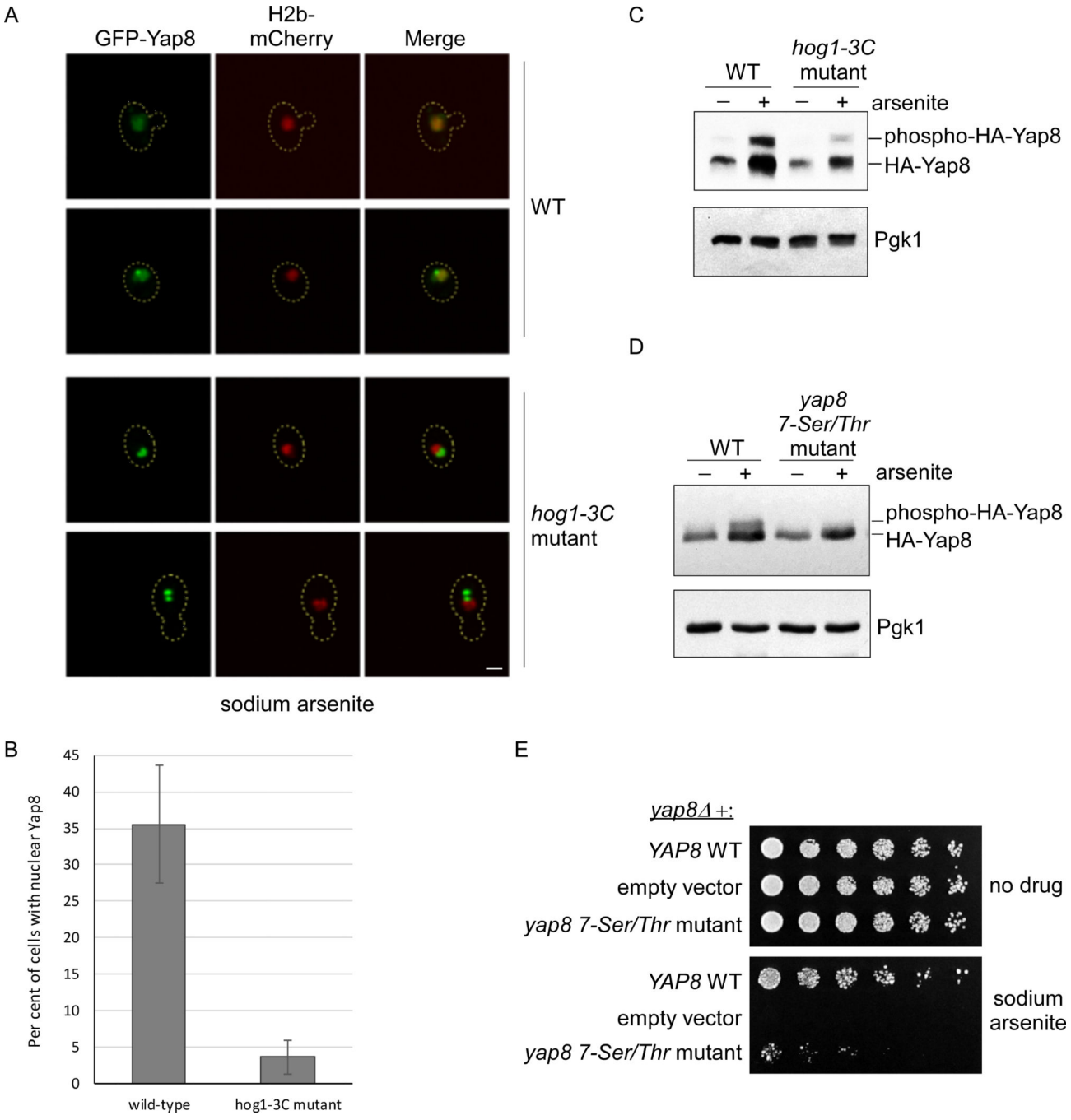

Fig. 4. Hog1 regulates multiple aspects of Yap8 function.

(**A**) Fluorescence microscopy showing GFP-Yap8 and the nuclear marker mCherry-tagged histone H2B after treating yeast with sodium arsenite (1 mM for 1 h). Cell outlines (yellow) were obtained from corresponding brightfield images. Scale bar, 2 μm. Similar results were obtained in at least three experiments. (**B**) Quantification of GFP-Yap8 nuclear localization in *hog1Δ* cells expressing WT Hog1 or Hog1–3C. 135 consecutive cells were counted in groups of 45 for each strain. Error bars indicate standard deviations. (**C**) Lysates from arsenite-treated (1 mM for 1 h) *hog1Δ* cells expressing HA-tagged Yap8 plus either WT

Hog1 or Hog1–3C og1were separated on a Phos-tag gel and immunoblotted for HA. Pgk1 is a loading control. Similar results were obtained in at least three experiments. (**D**) *yap8Δ* cells expressing WT Yap8 or the 7Ser/Thr mutant form of Yap8, in which 7 serine and threonine residues were mutated to alanine (Ser^{14}, Thr^{16}, Thr^{138}, Ser^{141}, Ser^{145}, Ser^{282}, and Ser^{292}). Similar results were obtained in at least two experiments. (**E**) Growth of *yap8Δ* cells expressing WT Yap8, an empty vector, or the Yap8 7-Ser/Thr mutant in the presence of arsenite (0.25 mM) cultured for 2–3 days. Similar results were obtained in two experiments.

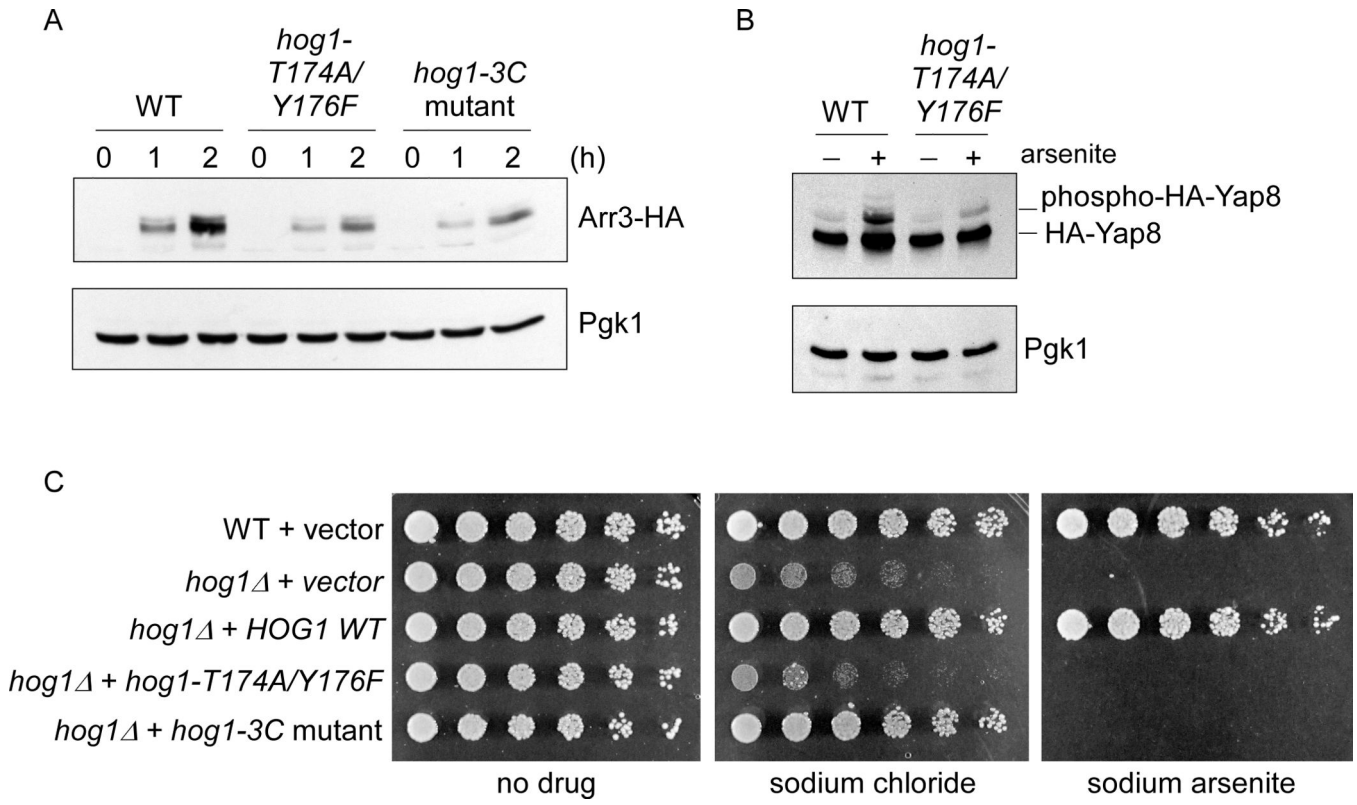

Fig. 5. Regulation of Yap8 by Hog1 requires both phosphorylation and thiol-based mechanisms.

(**A**) Immunoblotting for HA in lysates of arsenite-treated (1 mM) *hog1Δ* cells expressing WT Hog1, Hog1-T174A/Y176F, or Hog1–3C in addition to HA-tagged Arr3 from the endogenous locus. Pgk1 is a loading control. Similar results were obtained in more than three experiments. (**B**) Lysates of arsenite-treated *hog1Δ* cells expressing HA-tagged Yap8 and either WT Hog1 or Hog1-T174A/Y176F were separated on a Phos-tag gel and immunoblotted for HA. Pgk1 is a loading control. Similar results were obtained in three experiments. (**C**) *yap8*Δ cells expressing the indicated proteins were spotted in three-fold serial dilutions onto plates containing no drug, sodium chloride (0.4 mM), or sodium arsenite (1 mM) and cultured for 3–4 days. Similar results were obtained in at least three experiments (see also Fig. 1A and fig. S1).

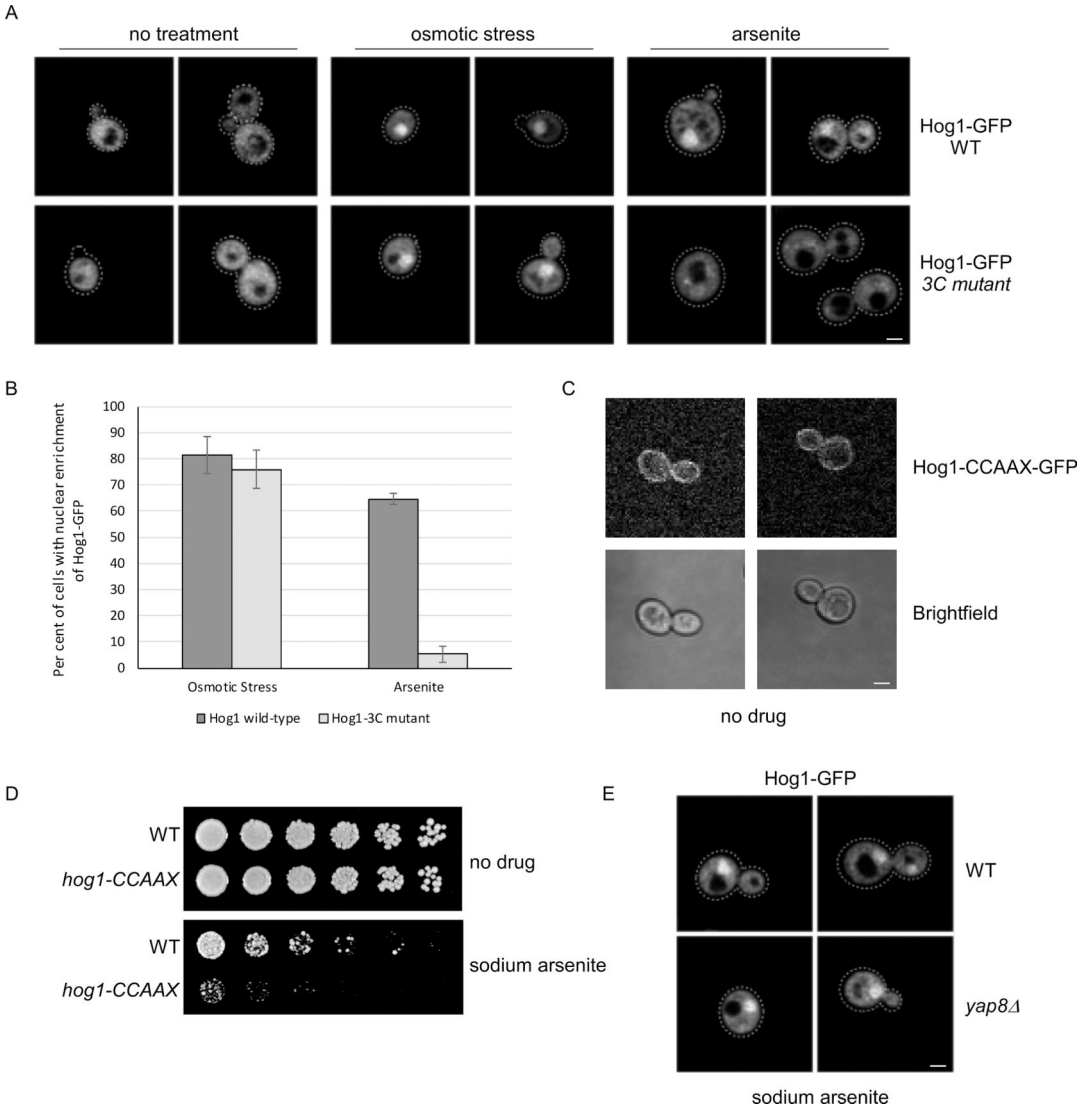

Fig. 6. Regulation of Hog1 subcellular localization by arsenic.

(**A**) Fluorescence microscopy showing GFP-tagged WT Hog1 and Hog1–3C in *hog1Δ* cells after treatment with sodium chloride (0.4 M for 30 min) or sodium arsenite (1 mM for 30 min). Cell outlines were obtained from corresponding brightfield images. Scale bar, 2 μm. Similar results were obtained in at least three experiments. (**B**) Quantification of Hog1-GFP nuclear localization as in (A). Three groups of 50 cells each were assessed for Hog1 nuclear localization. Error bars reflect standard deviations from these three groups. (**C**) Fluorescence microscopy showing GFP-tagged Hog1-CCAAX, which localizes to the plasma membrane (2). Corresponding brightfield images are shown. Scale bar, 2 μm. Similar results were obtained in three experiments. (**D**) Growth of *hog1*Δ cells expressing WT Hog1 or membrane-tethered Hog1-CCAAX on plates containing or lacking sodium arsenite (1.5 m). Cells were spotted in three-fold serial dilutions and cultured for 2–3 days. Similar results were obtained in three experiments. (**E**) Fluorescence microscopy showing WT Hog1-GFP in arsenite-treated (1 mM for 30 min) WT and *yap8Δ* strains. Cell outlines were obtained

from corresponding brightfield images. Scale bar, 2 μm. Similar results were obtained in three experiments.

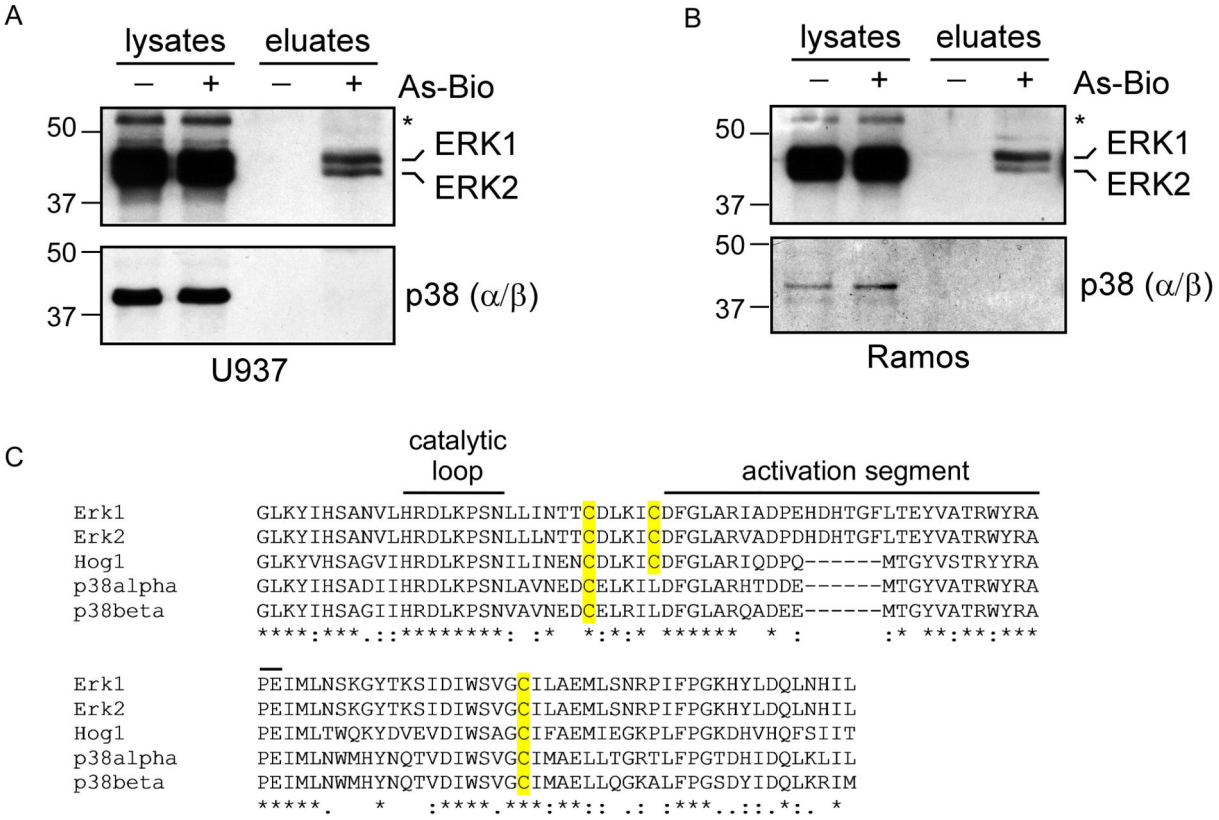

Fig. 7. Arsenic binding is a conserved feature of some mammalian MAPKs.

(**A-B**). Lysates of U937 (A) and Ramos (B) cells were treated with biotinylated arsenic (As-Bio; 20 μM), affinity purified for biotin, separated on Phos-tag gels, and immunoblotted for ERK1/2 and p38α/β. Asterisks indicate non-specific bands. Similar results were obtained in two experiments for each cell line. (**C**) Sequence analysis of yeast Hog1 and the four indicated human MAPKs. The catalytic loop and activation segment are indicated. The key cysteine residues corresponding to yeast Cys^{156}, Cys^{161}, and Cys^{205} are highlighted in yellow. Alignment was by Clustal Omega. Asterisks, identical residues; double dots, highly similar residues; single dots, similar residues.